Electronic Supplementary Material (ESI) for Environmental Science: Water Research & Technology.

Electronic Supporting Information: Exceptional Sorption Behavior of Porous Tungsten Oxide for Aqueous Lead

Cory K. Perkins, Travis M. Reed, Zachary A. Brown, and Allen W. Apblett*

Department of Chemistry, Oklahoma State University, Stillwater, Oklahoma 74078

EXPERIMENTAL

A previously reported method for making thermally stable mesoporous WO_3 thin-films was adapted to prepare porous WO_3 for this contribution.[1,2] Peroxopolytungstic acid was synthesized by dissolving H_2WO_4 in 30% H_2O_2. A mass of 5.0 g of H_2WO_4 powder (Alfa) was dispersed in a mixture of 20 mL of 18-MΩ H_2O and 35 mL of 30% H_2O_2 (Macron). The reaction mixture was magnetically stirred at 40 °C overnight, producing a pale yellow solution. The solution was then dried at 40 °C, yielding brightly colored yellow needle-like crystals. From the collected crystals, 1.0 g was dissolved in a mixture of 5.0 g H_2O, 3.0 g of 30% H_2O_2, and 1.0 g of ethanol. In a separate flask, the surfactant solution was prepared by dissolving 0.2 g of Brij-56 in ethanol. Once the reactants were dissolved, the two solutions were thoroughly mixed and the solution was allowed to slowly evaporate. The synthetic procedure is very attractive since there is no loss in mass of tungsten during the synthesis of the sorbent.

Instead of thermally removing the surfactant from the resultant powder, we used soxhlet ethanol extraction. By removing the organics with ethanol, rather than pyrolysis, the integrity of the pores were more likely to be maintained, yielding high surface area and a lower chance of carbon contamination. To confirm the presence of pores, we analyzed the surface area by nitrogen physisorption using a NOVA Quantachrome 4200e BET.

X-ray diffraction of the material before and after treatment of aqueous Pb^{2+} was carried out using a Bruker D8-A25-Advance X-ray diffractometer equipped with a LynxEye detector. Scanning electron micrographs of the solids before and after treatment were recorded using a FEI Quanta 600 field emission gun environmental scanning electron microscope. Raman spectra of the sorbent after solution-treatment were recorded on a Nicolet NXR 9610 Raman spectrometer. The starting material was embedded and sectioned with a microtome and analyzed by TEM using a JEOL JEM-2100 transmission electron microscope.

The concentration of Pb^{2+} during the sorption kinetics experiment was monitored using a Varian GTA120/AA240Z graphite furnace atomic absorption spectrometer (GFAAS) equipped with an auto sampler. A NIST-traceable 100 mg/L Pb^{2+} standard (BDH ARISTAR) was used to prepare the standard solutions used for GFAAS analysis. Aliquots of the treated samples were taken at regular time intervals and diluted to the appropriate concentrations with a solution of 1% HNO_3. The 1% nitric acid solution was made using trace metal grade HNO_3 from Mallinckrodt. For the kinetic study, we used approximately 40 mL of a 107 ppm Pb^{2+} solution to monitor the analyte concentration at various time intervals when treated with five different sorbent loadings.

An uptake capacity study was also performed to determine the maximum uptake of lead by the WO_3 sorbent. Roughly, 0.3 g (1.3 mmol) of the porous-WO_3 powder was used to treat a solution containing a large excess Pb^{2+} (30.0 mL of a 0.075 M solution), a molar ratio of Pb:WO_3 of 1.73:1, respectively. SEM, TEM, Raman, and XRD were used to characterize the resultant materials.

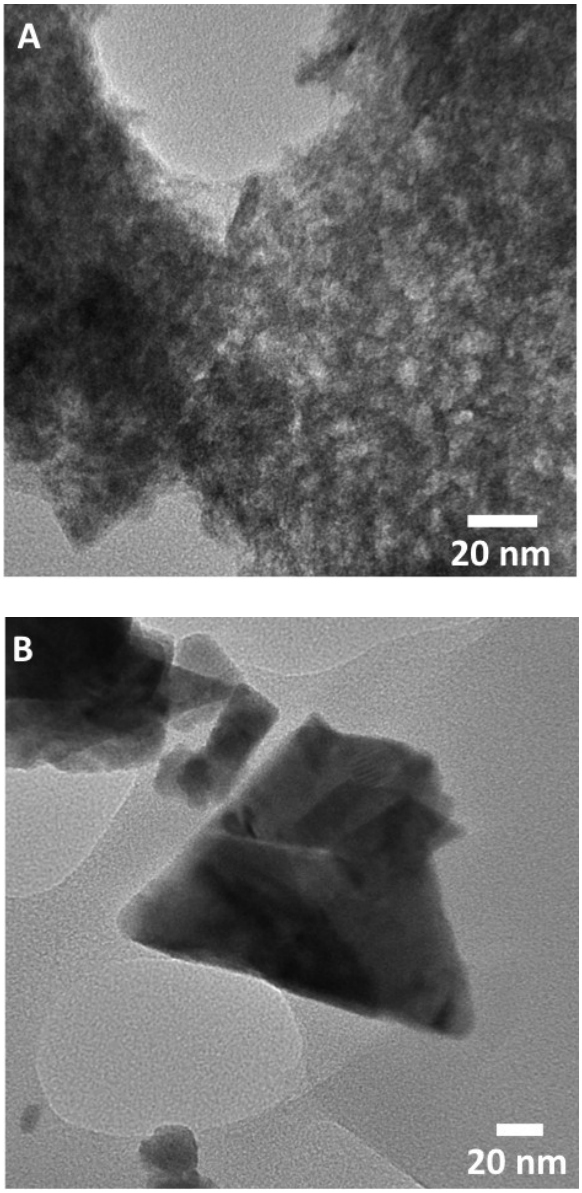

Figure S1. TEM Image of the porous WO_3 before (a) and after treatment with lead (b)

Sorption Kinetics for Mesoporous-WO_3

The sorption uptake curves (Figure S2) depicts an extremely fast sorption process in which the majority of the Pb^{2+} was removed within the first 15 minutes. For the highest loading,

0.260 mmol, the sorption capacity was reached in roughly 10 minutes, where the lowest mass loading, 0.093 mmol, somewhere between 30 and 90 min. The sorption capacities of the mesoporous materials were also very high, with very low mass loadings, highlighting the material's high affinity for the analyte. Because of the high affinity for Pb^{2+}, the reactions were with only a small molar excess of WO_3 to Pb^{2+}, from 3 to 10 times, where the commercially available nano-WO_3 had an excess range from 30-100. Furthermore, the sorption process was able to remove the concentration of Pb^{2+} from these solutions to below the instrumental detection limit of 0.5 ppb.

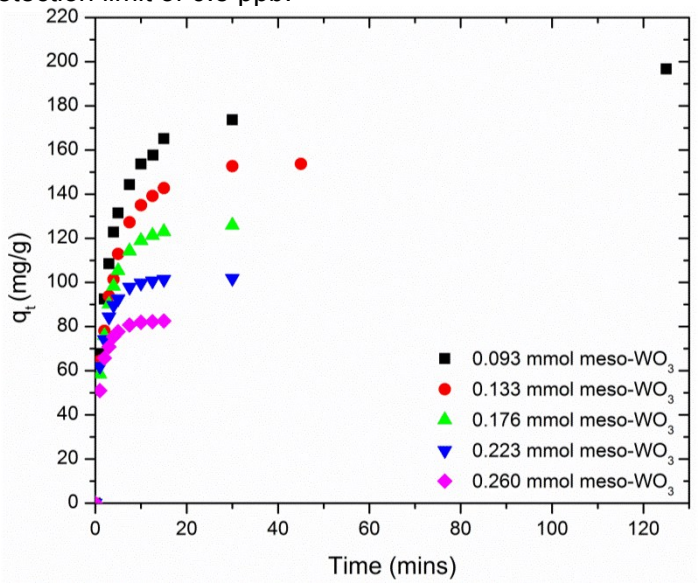

Figure S2. Sorption uptake curve for Pb^{2+} by mesoporous-WO_3

Lagergren first described the pseudo first-order rate expression in 1898, where k_1 is the kinetic rate constant for the pseudo first-order sorption process. The amount of analyte sorbed at any specific time (t) is represented by q_t and the amount of analyte sorbed at equilibrium is represented by q_e.[3]

$$q_t = q_e(1 - e^{-k_1 t}), \quad \text{(Eq 1).}$$

To simplify the natural log was taken giving a linear equation represented by

$$\ln(q_e - q_t) = \ln(q_e) - k_1 t, \quad \text{(Eq 2).}$$

From this equation, the values of k_1 and q_e can be determined from the slope and y-intercept, respectively, by the linear pseudo first-order plot. The results from the linear pseudo first-order model were better for the larger mass loadings. Figure S3 shows an obvious deviation from linearity for the lowest mass loading, corresponding to a lower correlation coefficient (R^2) summarized in Table S1. The experimental values of the equilibrium capacities were twice that of the predicted values from this model, suggesting it is not appropriate to use to model this process.

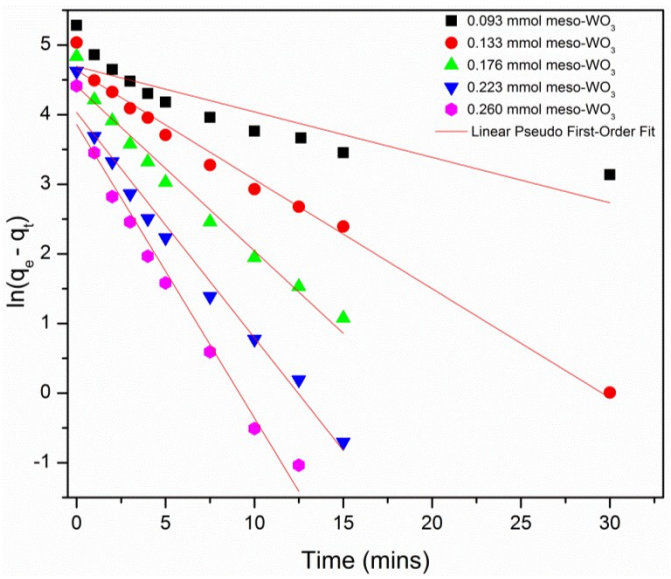

Figure S3. Linear Pseudo First-Order Fit for the Mesoporous-WO_3 Uptake of Pb^{2+}

Table S1. Kinetic Data from the Linear Pseudo First-Order Fit for the Mesoporous-WO_3

WO_3 (mmol)	k_1 (min^{-1})	q_e (mg/g)	q_e (mg/g) (experimental)	R^2
0.093	6.53×10^{-2}	109	197	0.765
0.133	1.57×10^{-1}	103	154	0.985
0.176	2.37×10^{-1}	81.8	126	0.971
0.223	3.24×10^{-1}	56.3	102	0.974
0.260	4.22×10^{-1}	47.3	82.6	0.973

The sorption fit using the pseudo second-order function, Figure S4, shows good fits throughout the mass loadings, even for the lowest mass loading. Table S2 shows the observed q_e values for this process are consistent with the predicted values from the function. Further, the R^2 values for this model all very high (R^2>0.99) suggesting this may be the best method for modeling this sorption process.

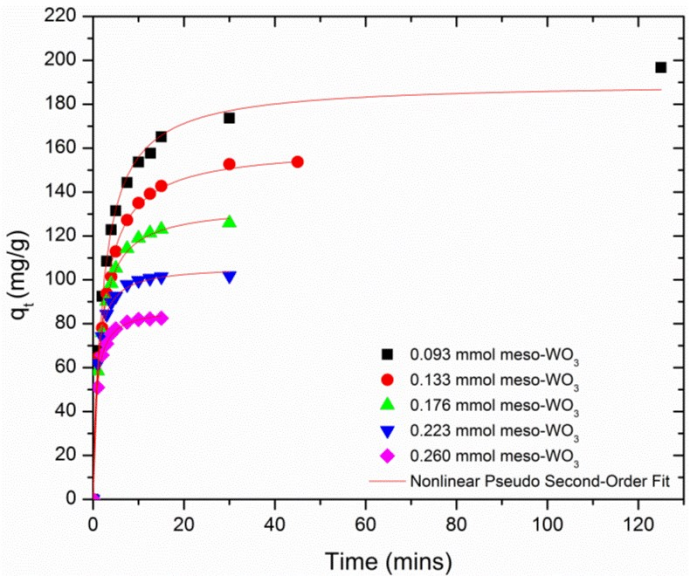

Figure S4. Nonlinear pseudo second-order fit for the mesoporous-WO_3 uptake of Pb^{2+}

Table S2. Kinetic Data from the Nonlinear Pseudo Second-order Fit for the Mesoporous-WO_3

WO_3 (mmol)	k_2 (g/mg min)	h (mg/g min)	q_e (mg/g)	q_e (mg/g) (experimental)	R^2
0.093	2.42×10^{-3}	87.25	190	197	0.993
0.133	3.12×10^{-3}	80.60	161	154	0.991
0.176	5.32×10^{-3}	95.59	134	126	0.998
0.223	1.23×10^{-2}	139.5	106	102	0.998
0.260	1.67×10^{-2}	127.8	87.4	82.6	0.999

Finally, the sorption process was modeled using the linear pseudo second-order model (Figure S5). The data from this model (Table S3) has almost perfect correlation coefficients and q_e values that are very close to the observed values, only slightly overestimating the values in each case. There has been some concern raised to the validity of using the linear pseudo-second order model, due to a spurious correlation.[4]

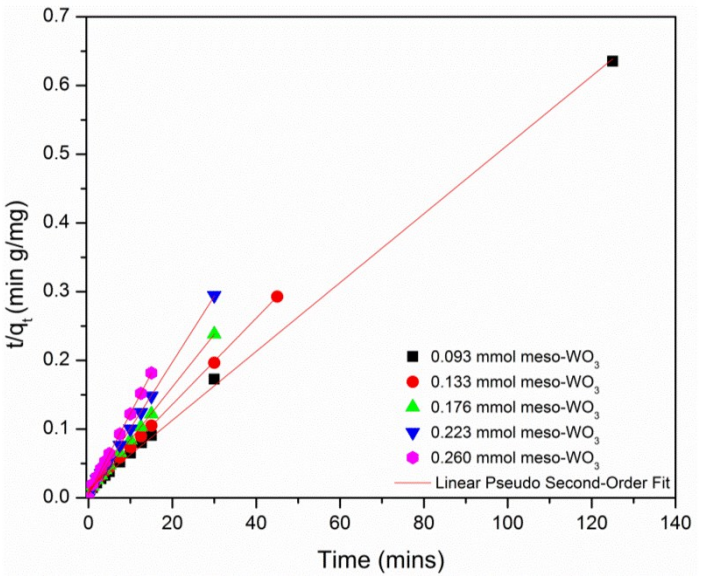

Figure S5. Linear pseudo second-order fit for the mesoporous WO_3 uptake of Pb^{2+}

Table S3. Kinetic Data from the Linear Pseudo Second-Order Fit for the Mesoporous -WO_3

WO_3 (mmol)	k_2 (g/mg min)	h (mg/g min)	q_e (mg/g)	q_e (mg/g) (experimental)	R^2
0.093	1.96×10^{-3}	78.2	200	197	1.00
0.133	2.45×10^{-3}	62.3	159	154	0.999
0.176	7.43×10^{-3}	126	130	126	0.999
0.223	1.85×10^{-2}	200	104	102	1.00
0.260	2.61×10^{-2}	189	85.0	82.6	0.999

References:

(1) Wang, W.; Pang, Y.; Hodgson, S. N. B. *J. Sol-Gel Sci. Technol.* **2011**, *58* (1), 135–141.
(2) Wang, W.; Pang, Y.; Hodgson, S. N. B. *Microporous Mesoporous Mater.* **2009**, *121* (1), 121–128.
(3) Lagergren, S. *K. Sven. Vetenskapsakademiens. Handl.* **1898**, *24* (4), 1–39.
(4) Zhang, J.-Z. *Chem. Commun.* **2011**, *47* (24), 6861–6863.